15 August 2002

Optics Communications 209 (2002) 265–271

OPTICS COMMUNICATIONS

www.elsevier.com/locate/optcom

# Efficient conversion of a Gaussian beam to a high purity helical beam

Galina Machavariani[a,*], Nir Davidson[a], Erez Hasman[b], Shmuel Blit[a], Amiel A. Ishaaya[a], Asher A. Friesem[a]

[a] *Department of Physics of Complex Systems, Weizmann Institute of Science, Rehovot 76100, Israel*
[b] *Optical Engineering Laboratory, Faculty of Mechanical Engineering, Technion-Israel Institute of Technology, Haifa 32000, Israel*

Received 13 November 2001; received in revised form 13 February 2002; accepted 5 June 2002

**Abstract**

A method for efficiently converting a Gaussian beam into a helical Laguerre–Gaussian (LG) beam is presented. It is based on using a pair of axicons to produce a shifted-Gaussian (doughnut) intensity distribution that is then passed through a spiral phase element. It is shown that the conversion efficiency can be as high as ~98%, and the calculated far-field intensity distributions of the output beams are very close to those of corresponding pure LG intensity distributions. The principle of the method, the needed optical arrangement, and calculated and experimental results are presented. 

*PACS:* 41.85.Ct; 41.85.Ew; 42.60.Jf

*Keywords:* Helical beams; Beam conversion; Phase elements; Laser beams

## 1. Introduction

In recent years, the formation of laser beams with phase singularities has attracted considerable interest [1–15]. Typically, the field of such beams is *helical* (or spiral) with an azimuthal angular dependence given by $\exp(\mathrm{i}l\phi)$. Helical laser beams have been exploited for trapping of atoms and macroscopic particles [2,3], focusing of atomic beams [4], transferring of orbital angular momentum to macroscopic objects [1,5,6], rotational frequency shifting [7], mode transformation with non-linear frequency doubling [8], and switching helicities as a means of information processing [9].

The helical field distribution can be described in terms of non-degenerate $(p,l)$ Laguerre–Gaussian (LG) modes, as

$$U_{p,l}^{\mathrm{LG}}(r,\phi) = U_0\,\rho^{|l|/2}L_p^{|l|}(\rho)\exp(-\rho/2) \times \exp(\mathrm{i}l\phi), \tag{1}$$

where $r$ and $\phi$ are the cylindrical coordinates, $\rho = 2r^2/w^2$, the waist $w$ is the radius for which the Gaussian term falls to $1/e$ of its on-axis value, and

* Corresponding author. Fax: +972-8-934-4109.
*E-mail address:* galina@wisemail.weizmann.ac.il (G. Machavariani).

0030-4018/02/$ - see front matter 
PII: S0030-4018(02)01683-8

$L_p^{|l|}$ are the generalized Laguerre polynomials of order $p$ and index $l$. The index $l$ may be positive or negative, and the modes of opposite $l$ lead to opposite helical phase having the same radial intensity distribution. In general, the intensity distribution of the LG $(p, l)$ mode will have a circularly symmetric annular shape.

Laguerre–Gaussian high order modes can be generated inside a laser cavity, so the output beam will have a helical field distribution. For example, circular symmetric $(0, 1)$, $(0, 2)$ and $(0, 3)$ doughnut helical modes where produced by coherent intracavity coupling and recombination of two non-helical modes (produced by suitably selected absorbers and apertures inside the resonator) [10]. Specific helical modes can be selected by inserting of spiral phase elements (SPE) into the laser cavity [11]. It is also possible to convert a high-order Hermite–Gaussian mode of indices $m$ and $n$ into a pure LG mode with $p = \min(m, n)$ and $l = m - n$. This was done with two cylindrical lenses and appropriate use of the Gouy phase shift [6].

Alternatively, a helical beam can be obtained directly from a Gaussian one, outside the laser cavity, by means of computer-generated holograms [12,13] and SPE [14,15]. However, the resulting helical beam is not pure, whereby it contains a superposition of different LG modes; it was reported that the power contains less than 80% of the desired helical mode power, whereas the rest of the power is in other high order LG modes [12–15].

The purity of the LG beams is of high importance, because the intensity pattern of a pure free-space mode does not change as it propagates. In contrast to this, the intensity distribution of a beam composed of several modes, does change as it propagates. This may be of particular importance in optical fiber communication systems where high-order modes are used, for example, for chromatic dispersion compensation, and undesired modes must be strongly suppressed. For such applications, the LG beams of lower purity, such as those produced with the aid of holograms, are inadequate. Moreover, with holograms, it is necessary to limit the intensity of the beams, because of the low damage threshold of holographic materials.

With SPEs, the degradation in the efficiency of conversion from a Gaussian to a desired helical beam is due to the different intensity distributions. Specifically, the efficiency increases as the difference in the intensity distributions of the original and desired helical beam decreases. The principle of reshaping intensity before applying a phase correction to produce a desired field, have being exploited in a wide range of contexts [16].

In this paper we determine the conditions for obtaining the highest possible efficiency for converting a normal Gaussian beam directly to a desired helical one, with the aid of SPEs. In addition, we develop a new method in which we obtain even higher conversion efficiency. In this method, the Gaussian beam is first converted to a "shifted-Gaussian" (doughnut) beam, and thereafter to a desired helical beam with the aid of SPE. The method is validated with a series of experiments to obtain helical beams having the distribution of LG $(0, 1)$ and $(0, 2)$ modes. The theoretical and experimental procedures and results are presented in the following sections.

## 2. Conversion efficiency

A common technique for obtaining a beam with a desired helicity is to start with the fundamental Gaussian beam and convert it to a helical one by means of phase element with desired $\exp(\mathrm{i}l\phi)$ helicity. Unfortunately, the field distribution of the resultant beam does not represent a pure mode. Specifically, the helical LG modes $U_{pl}^{\mathrm{LG}}$ form a complete set of functions, whose expansion coefficients are

$$C_{00,pl} = \frac{\int\int U_{pl}^{\mathrm{LG}*} \exp(\mathrm{i}l\phi) U_{00}^{\mathrm{LG}} \,\mathrm{d}\phi r \,\mathrm{d}r}{2\pi\sqrt{\int (U_{pl}^{\mathrm{LG}})^* U_{pl}^{\mathrm{LG}} r \,\mathrm{d}r \int (U_{00}^{\mathrm{LG}})^2 r \,\mathrm{d}r}}. \tag{2}$$

The relative weight of the specific LG mode with indices $(p,l)$ in the overall intensity of the resultant beam is

$$I_{00,pl} = |C_{00,pl}|^2. \tag{3}$$

Using Eqs. (1) and (3), we calculated the relative weights of the modes $U_{01}^{\mathrm{LG}}$, $U_{02}^{\mathrm{LG}}$ and $U_{03}^{\mathrm{LG}}$ in beams converted from a normal fundamental Gaussian

beam, as a function of the waist parameter $w$ of the corresponding LG modes. The conversion to $U_{0l}^{LG}$ is done with SPE having the phase $\exp(il\phi)$ with $l = 1, 2, 3$. The waist parameter $w$ of the individual mode is expressed in units of $w_{00,}$ which is the waist of the incident Gaussian beam. The results are presented in Fig. 1. As evident, the choice of $w = w_{00}$, which provides conversion efficiencies of 78.5% for $l = 1$ and 50% for $l = 2$ [12,15], does not give maximal efficiency. Indeed, since the LG modes $U_{pl}^{LG}$ with any $w$ form a complete set, the real conversion efficiency of $U_{00}^{LG} \to U_{0,l}^{LG}$ transformation is higher, reaching 93% for $l = 1$, 84.4% for $l = 2$ and 77% for $l = 3$. Similar values were obtained for $l = 1$ and $l = 3$ by numerically optimizing the beam waist at the output for maximum overlap with the input Gaussian beam [17].

As pointed out, the conversion efficiency can be even higher if the difference in the intensity distributions of the incident and desired beams will be closer. This can be achieved with an incident beam whose intensity distribution is close to that of the $U_{0l}^{LG}$ modes. It can be obtained by radially "shifting" the normal fundamental Gaussian distribution to form an annular distribution with a Gaussian cross-section and nearly uniform phase. In practice, this can be realized, to a good approximation, with two axially separated axicons for providing the needed shift parameter $r_o$, as shown in Fig. 2. The resultant field distribution is approximately

$$E(r, \phi) = E_0 \exp(-(r - r_0)^2 / w_{00}^2)), \tag{4}$$

also confirmed by numerical solutions of the Fresnel integrals for a Gaussian beam impinging an axicon [18].

To justify the use of the approximate formula (4), we first performed precise numerical calculations, using Fresnel diffraction integrals [19], to determine the intensity and phase profile of an incident Gaussian beam after it passes a pair of axicons, for different propagation distances and different axicon's base angles. Then, we calculated the relative weight of the intensity of specific LG modes, as well as of a shifted-Gaussian beam (4), in the overall intensity of the final output beam. We found that the relative weight of the pure (0, 1) LG mode (with optimized waist) in the far field intensity of the output beam is 97.8% (when the slope of the axicons was 0.0042, the refractive index was 1.5 and the wavelength was 1.064 μm), while the relative weight of the shifted-Gaussian beam is 97.2%. These results imply that use of the simpler "shifted-Gaussian" (4) would approximately lead to the desired beam.

We calculated the relative weights of the pure $U_{0l}^{LG}$ modes for $1 \leqslant l \leqslant 5$ in beams, converted from

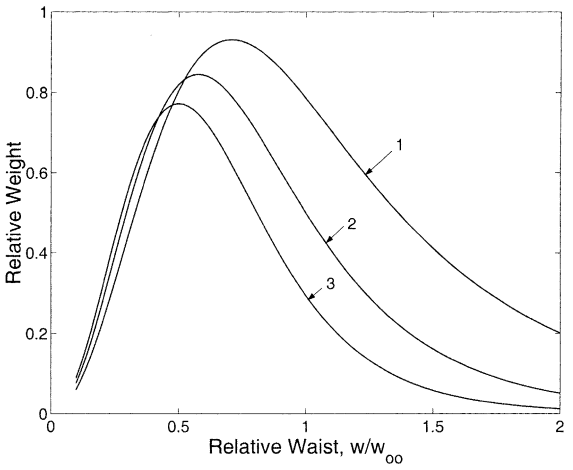


Fig. 1. The relative weights of pure LG modes in the output beam after passing a normal Gaussian beam through SPEs, as function of the relative waist parameter. (1) Relative weight of pure LG (0, 1) mode after passing through $\exp(i\phi)$ SPE; (2) relative weight of pure LG (0, 2) mode after passing through $\exp(i2\phi)$ SPE; (3) relative weight of pure LG (0, 3) mode after passing through $\exp(i3\phi)$ SPE. The horizontal axis is the waist parameter of corresponding (0, 1), (0, 2) or (0, 3) LG mode, in the units of the waist $w_{00}$ of the incident Gaussian beam.

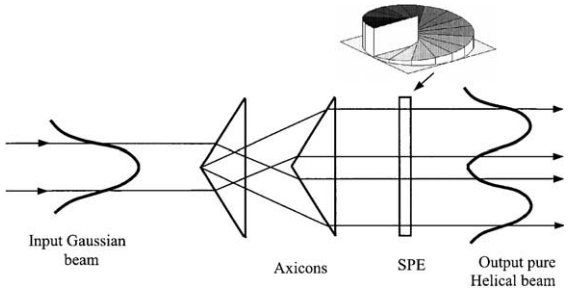


Fig. 2. The experimental configuration for efficient beam conversion. The intensity distributions of the incident and outgoing beams are drawn by solid curve.

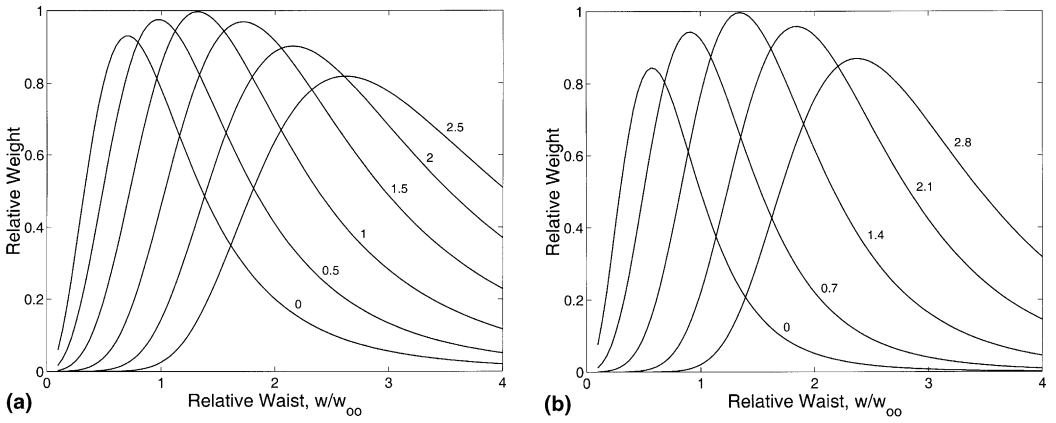


Fig. 3. The relative weights of pure LG modes in the output beam after passing a *shifted-Gaussian* (doughnut) beam through SPEs, as function of the relative waist parameter. (a) Relative weight of pure LG $(0,1)$ mode after passing through $\exp(i\phi)$ SPE; (b) relative weight of pure LG $(0,2)$ mode after passing through $\exp(i2\phi)$ SPE. The horizontal axis is the waist parameter of corresponding pure LG mode, in the units of the waist $w_{00}$ of the incident Gaussian beam. The different curves are plotted for different shifting parameter $r_o$, which is denoted near each curve in the units of $w_{00}$.

"shifted-Gaussian" beam (Eq. (4)), as a function of the relative waist parameter $w/w_{00}$, for different shifting parameter $r_0$. The results obtained for $l = 1$ and $l = 2$ are presented in Fig. 3. Fig. 3(a) shows the relative weights of the pure LG $(0,1)$ distribution in the output beam for which the $\exp(i\phi)$ SPE was used. Fig. 3(b) shows the relative weights of the pure LG $(0,2)$ mode in the output beam for which the $\exp(i2\phi)$ SPE was exploited. The different curves are obtained for different shift parameters $r_o$, which are indicated adjacent to the curves in the units of $w_{00}$. The waist parameter $w$ of desired pure mode is denoted on the horizontal axis in units of $w_{00}$. The optimal shift parameter $r_o$ gives the maximal conversion efficiency and yields 0.982 $w_{00}$ for $U_{0l}^{LG}$ and 1.436 $w_{00}$ for $U_{02}^{LG}$ . The optimal $w$ parameters of the desired mode distributions are 1.3065 $w_{00}$ for $U_{0l}^{LG}$ and 1.3689 $w_{00}$ for $U_{02}^{LG}$. As evident, the relative weights, namely, conversion efficiencies, obtained with approximate formula (4), can reach very high values. More accurate calculations, based on Fresnel diffraction integrals [19], with a Gaussian beam passing through two axicons and SPE, yield 97.8% with $\exp(i\phi)$ SPE and 95% with $\exp(i2\phi)$ SPE. These values are substantially higher than those obtained by directly converting a Gaussian beam to a helical one, where according to Fig. 1 the conversion efficiencies are 93% with $\exp(i\phi)$ SPE and 84.4% with $\exp(i2\phi)$ SPE.

## 3. Experimental procedure and results

In order to evaluate our conversion method, we performed experiments with CW Nd-YAG laser and pulsed Nd-YAG laser. The experimental arrangement is shown in Fig. 2. The waist $w_{00}$ of the incident Gaussian beam on the first axicon was about 3 mm; we chose this relatively large waist radius in order to minimize the effect of imperfection at the tip of the axicon. Both axicons had 50 mRad base angle and no AR coating. The distance between two axicons defines the shift parameter $r_0$, and was adjusted to match the radius of the corresponding doughnut in the specific helical LG mode (see Fig. 3). Two typical transmittive spiral phase elements were used [11]. One, which changes the phase of the wavefront by $\exp(i\phi)$ $(l = 1)$ in order to obtain the $U_{01}^{LG}$ distribution, and other, which changes the phase by $\exp(i2\phi)(l = 2)$ in order to obtain the $U_{02}^{LG}$ distribution. The phase elements were fabricated from fused silica as multilevel surface relief elements with 32 phase levels. This high number of levels is necessary in order to obtain diffraction efficiency

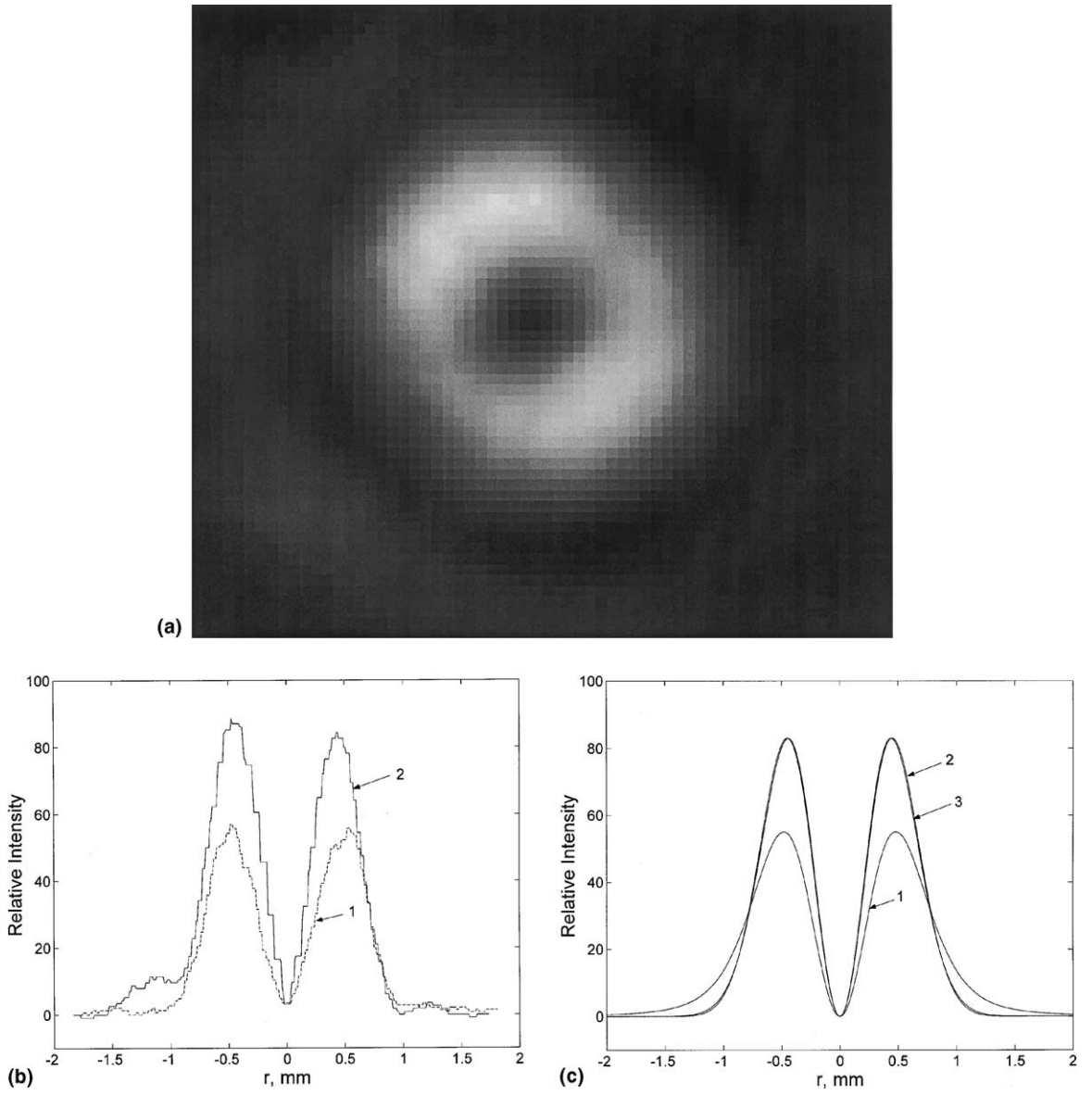


Fig. 4. Intensity distributions of the helical beam at the far-field when passing the incident Gaussian and shifted-Gaussian beam through $\exp(i\phi)$ SPE; (a) experimental intensity distribution for a shifted-Gaussian incident beam; (b) experimental intensity cross-sections for a normal Gaussian incident beam (curve 1) and shifted-Gaussian incident beam (curve 2); (c) calculated far-field intensity cross-sections for a normal Gaussian (curve 1) and shifted-Gaussian (curve 2) incident beams, and pure (0, 1) LG intensity distribution (curve 3).

more than 99% [20]. The output beam intensity distribution passed through a spherical lens ($f = 101$ cm) and was detected by a CCD camera to obtain the far-field distribution, which was then evaluated with a Spiricon beam analyzer.

The results obtained for the far-field output intensity distributions are presented in Figs. 4 and 5. Fig. 4 shows the intensity distribution when passing the incident beams through an $\exp(i\phi)$ SPE. Fig. 4(a) shows a photograph of the detected in-

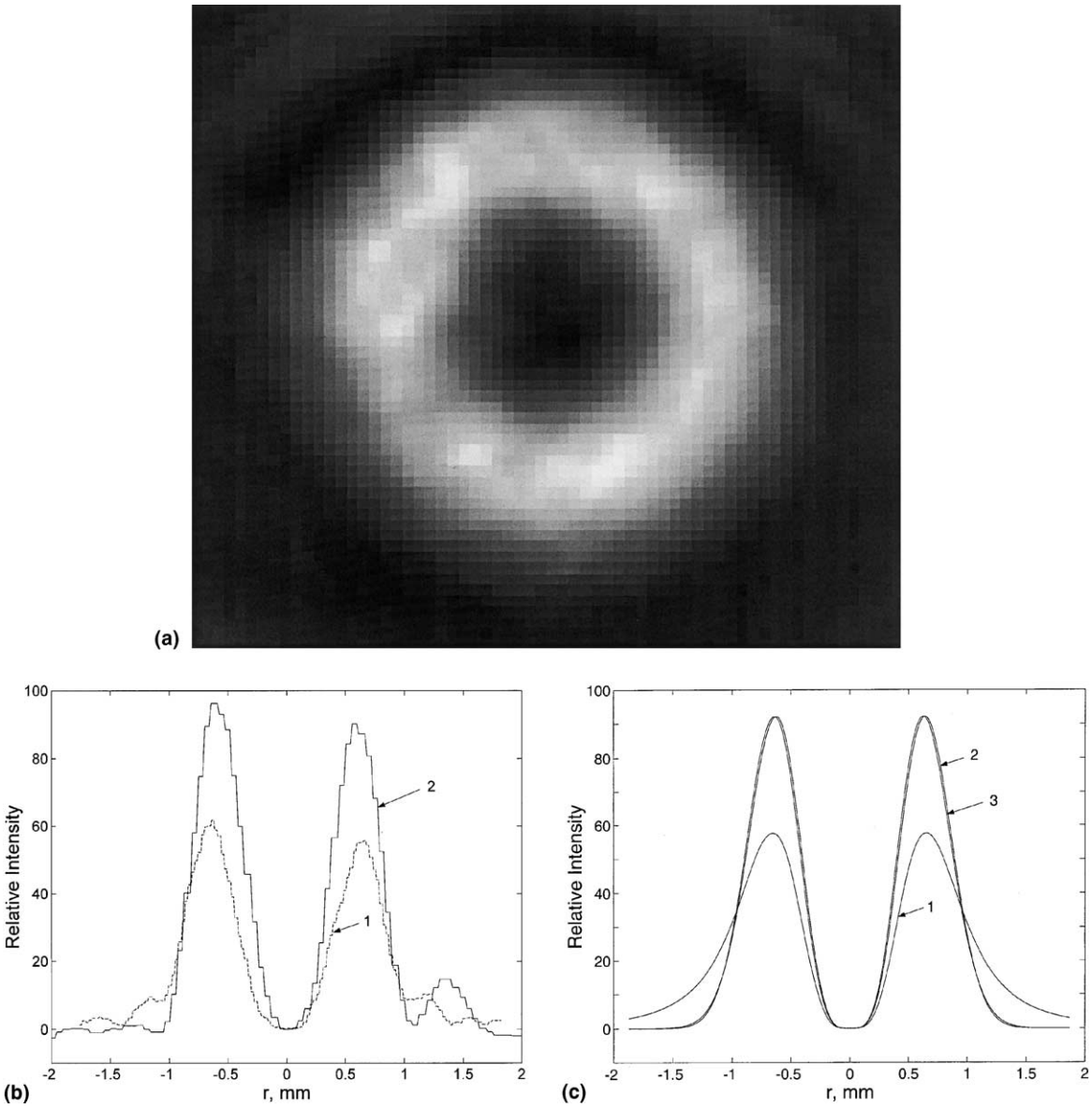


Fig. 5. Intensity distributions of the helical beam at the far-field when passing the incident Gaussian and shifted Gaussian beam through $\exp(i2\phi)$ SPE; (a): experimental intensity distribution for a shifted Gaussian incident beam; (b): experimental intensity cross-sections for a normal Gaussian incident beam (curve 1) and shifted Gaussian incident beam (curve 2); (c): calculated far-field intensity cross-sections for a normal Gaussian (1) and shifted Gaussian (2) incident beams, and pure (0, 2) LG intensity distribution (3).

tensity distribution when passing a shifted-Gaussian beam through the $\exp(i\phi)$ SPE. The expected doughnut shape is clearly evident. Fig. 4(b) shows the experimental cross-sections of the intensity distributions when using an incident Gaussian beam (curve 1) and an incident shifted Gaussian beam (curve 2). Fig. 4(c) shows the corresponding calculated intensity distributions, obtained by Bessel–Fourier transformation of the incident beams [19]. Also shown in Fig. 4(c) is the calculated pure LG (0, 1) intensity distribution (curve 3). Fig. 5 shows the intensity distribution when passing the

incident beams through an exp(i2$\phi$) SPE. Fig. 5(a) shows a photograph of the detected intensity distribution when passing a shifted-Gaussian beam through the exp(i2$\phi$) SPE. Again, the expected doughnut shape is clearly evident. Fig. 5(b) shows the experimental cross-sections of the intensity distributions when using an incident Gaussian beam (curve 1) and an incident shifted Gaussian beam (curve 2). Fig. 5(c) shows the corresponding calculated intensity distributions, obtained by Bessel–Fourier transformation of the incident beams [19]. Also shown in Fig. 5(c) is the calculated pure LG $(0, 2)$ intensity distribution (curve 3). As evident from these results, the intensity distributions when using a shifted Gaussian incident beams, are nearly identical to those of the pure LG distributions. This is not the case when using a normal Gaussian incident beam. Also, there is a reasonable agreement between the experimental and calculated results, albeit with some differences. We attribute these differences to imperfect axicons surfaces and tips, as well as to the absence of the anti-reflection coatings. Specifically, the surface figure of the axicons was about $\lambda$ at 514 nm, and the tip imperfection had a radius of about 0.4 mm. These deficiencies of the axicons also resulted in secondary lobes, as seen in the experimental results.

## 4. Concluding remarks

We presented a method for efficiently obtaining doughnut helical beams with high beam quality. Indeed the far field intensity distributions of the beams obtained by proposed method are very close to those of corresponding pure LG modes. Our method could be extended for obtaining both degenerate LG and Hermite–Gaussian intensity distributions. First, the intensity distributions of the original and desired beams should be matched and, second, the correct phase is introduced.

## Acknowledgements

This research was supported by Pamot Venture Capital Fund through Impala Ltd.

## References

[1] L. Allen, M.W. Beijersbergen, R.J.C. Spreeuw, J.P. Woerdman, Phys. Rev. A 45 (1992) 8185.
[2] T. Kuga, Y. Torii, N. Shiokawa, T. Hirano, Phys. Rev. Lett. 78 (1997) 4713.
[3] S. Sato, Y. Harada, Y. Waseda, Opt. Lett. 19 (1994) 1807.
[4] J.J. McCelland, M.R. Scheinfein, J. Opt. Soc. Am. B 8 (1991) 1974.
[5] H. He, M.E.J. Friese, N.R. Heckenberg, H. Rubinsztein-Dunlop, Phys. Rev. Lett. 75 (1995) 826.
[6] M.W. Beijersbergen, L. Allen, H.E.L.O. van der Veen, J.P. Woerdman, Opt. Commun. 96 (1993) 123.
[7] J. Courtial, D.A. Robertson, K. Dholakia, L. Allen, M.J. Padgett, Phys. Rev. Lett. 81 (1998) 4828.
[8] K. Dholakia, N.B. Simpson, M.J. Padgett, L. Allen, Phys. Rev. A 54 (1996) R3742.
[9] C. Tamm, C.O. Weiss, J. Opt. Soc. Am. B 7 (1990) 1034.
[10] M. Harris, C.A. Hill, J.M. Vaughan, Opt. Commun. 106 (1994) 161.
[11] R. Oron, N. Davidson, A.A. Friesem, E. Hasman, Opt. Commun. 182 (2000) 205.
[12] N.R. Heckenberg, R. McDuff, C.P. Smith, H. Rubinsztein-Dunlop, M.J. Wegener, Opt. Quantum Electron. 24 (1992) S951.
[13] J. Arlt, K. Dholakia, L. Allen, M.J. Padgett, J. Mod. Opt. 45 (1998) 1231.
[14] G.A. Turnbull, D.A. Robertson, G.M. Smith, L. Allen, M.J. Padgett, Opt. Commun. 127 (1996) 183.
[15] M.W. Beijersbergen, R.P.C. Coerwinkel, M. Kristensen, J.P. Woerdman, Opt. Commun. 112 (1994) 321.
[16] C.-Y. Han, Y. Ishii, K. Murata, Appl. Opt. 22 (1983) 3644.
[17] M.A. Clifford, J. Arlt, J. Courtial, K. Dholakia, Opt. Commun. 156 (1998) 300.
[18] R. Ozeri, L. Khaykovich, N. Friedman, N. Davidson, J. Opt. Soc. Am. B 17 (2000) 1113.
[19] J.W. Goodman, Introduction to Fourier Optics, McGraw-Hill, New York, 1968.
[20] E. Hasman, N. Davidson, A.A. Friesem, Opt. Lett. 16 (1991) 423.